The SiO_2 abundance on the surfaces of the Moon and Mercury

Renggli C.J., Morlok A., Weber I., Reitze M., Di Rocco T., Berndt J., Pack A., Hiesinger H.

https://doi.org/10.53480/bf74-m226

Supplementary Tables and Figures

Table S*1*. Major oxide compositions of the investigated glasses and the measured spectral positions of the respective CF. The ID Names refer to the IRIS database at https://iris.uni-muenster.de/.

Sample #		SiO_2	TiO_2	Al_2O_3	FeO	MgO	CaO	Totals	CF	ID/Name
		wt.%	wt.%	wt.%	wt.%	wt.%	wt.%	wt.%	µm	
C2	gl.1	97.6	0.0	0.7	0.9	0.9	0.5	100.6	7.41	732 syn lunar glass + C2
C2	gl.2	97.0	0.1	0.7	1.5	1.4	0.6	101.3	7.36	732 syn lunar glass + C2
C1		64.1	0.1	2.9	24.8	3.2	4.3	99.3	7.75	731 syn lunar glass + C1
C3		59.4	0.4	11.8	8.0	9.5	9.4	98.4	7.91	733 syn lunar glass + C3
D7		13.1	3.3	49.5	3.3	6.7	21.7	97.5	9.00	737 syn lunar glass + D7
C8b	gl.1	10.1	3.4	50.0	3.6	7.1	22.6	96.7	9.13	736 syn lunar glass + C8b
C8b	gl.2	10.1	3.4	50.0	3.6	7.1	22.6	96.7	9.15	736 syn lunar glass + C8b
D6		3.8	3.5	58.5	1.3	3.0	27.0	97.1	9.50	735 syn lunar glass + D6
D5	gl.1	0.5	7.0	56.6	0.0	0.1	33.0	97.1	9.86	734 syn lunar glass + D5
D5	gl.2	0.5	7.0	56.6	0.0	0.1	33.0	97.1	9.88	734 syn lunar glass + D5

Table S*2*. Fit coefficients, standard deviations of the coefficients and R^2 values for 2nd order and linear fit parameters for SiO_2 wt.% vs. CF position and 2nd order fit for SiO_2 mol% vs. CF position.

	Fit coefficients and standard deviations						
	a	SD a	b	SD b	c	SD c	R^2
SiO_2 wt.%, 2nd order polynomial	1.28e-4	3.2e-5	-3.55e-2	3.6e-3	9.649	9.9e-2	0.957
SiO_2 wt.% linear			-2.41e-2	1.7e-3	9.425	8.6e-2	0.926
SiO_2 mol% 2nd order polynomial	1.25e-4	2.3e-5	-3.66e-2	2.6e-3	9.741	7.7e-2	0.966

Table S*3*. Calculated landing site SiO_2 wt.% concentrations for lunar sample return missions over an area with a radius of 0.5° at each location. Histograms of these date are shown in Figures S4 and S5.

	A11	A12	A14	A15	A16	A17	L16	L20	L24	CE5	CE6
Ave.	46.2	46.6	48.8	47.7	51.0	48.5	45.7	49.7	45.6	45.9	47.0
Std.	0.7	0.6	0.7	1.3	0.9	1.5	0.6	0.8	0.7	0.6	0.7

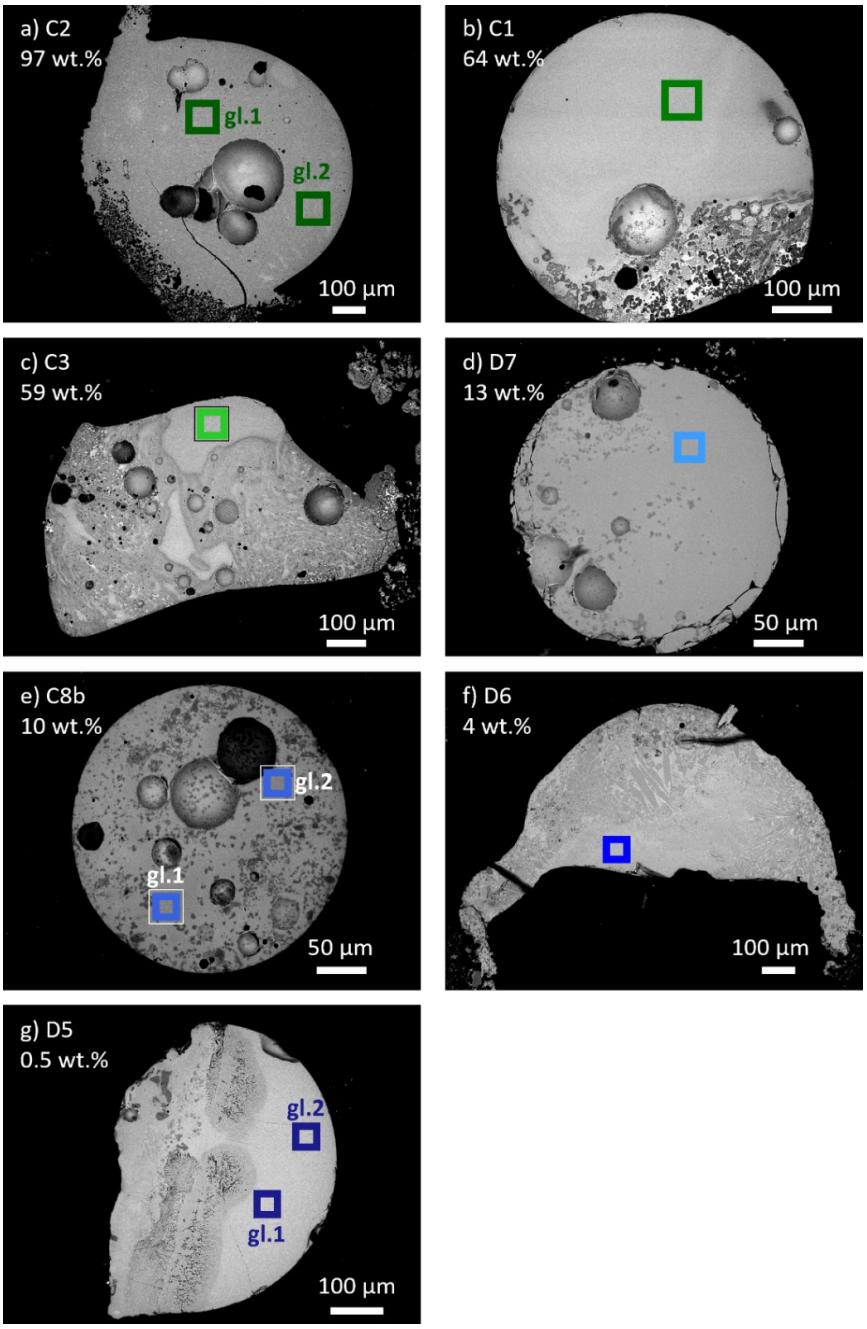

Figure S1. Back-scattered electron images of the synthetic glass samples investigated in this study from a) with the highest SiO_2 concentration of 97.6 wt.% to g) with the lowest SiO_2 concentration with 0.5 wt.%. No sample was fully homogenized but rather includes powder components on the rims from the starting material, parts of incomplete melting, or crystallization during quenching. The blue squares indicate the regions of analysis investigated in this paper. All these areas are chemically homogeneous, and fully glassy as shown in the Raman and FTIR spectra. Where two FTIR spectra were collected they are labelled as gl.1 and gl.2. the locations of the Raman spectra always correspond to the positions gl.1.

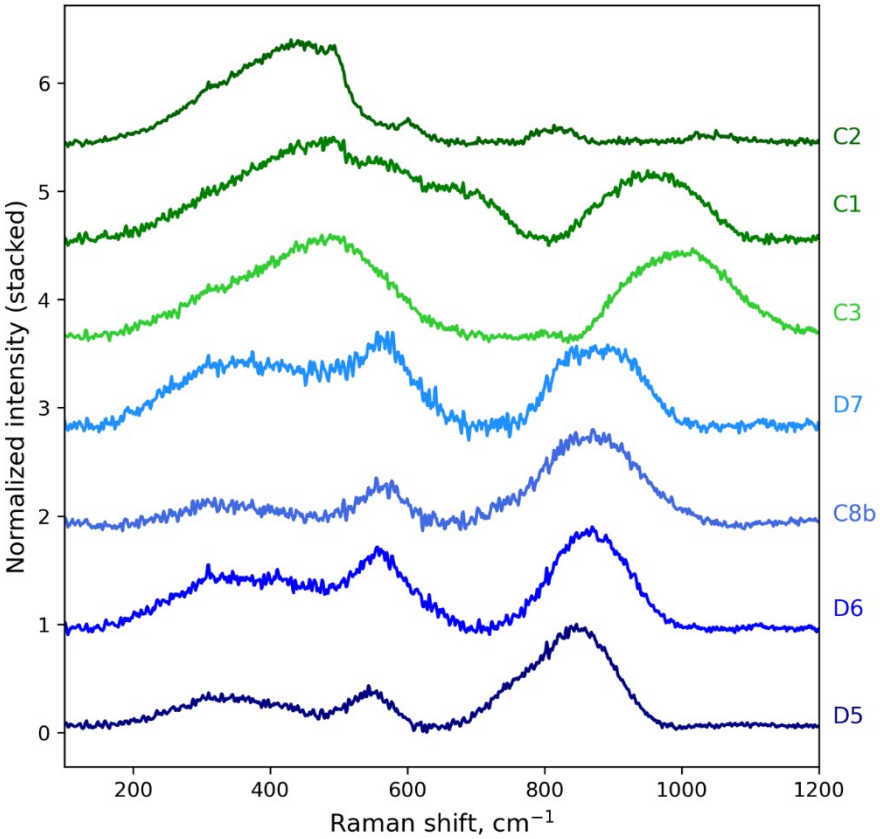

Figure S2. Raman spectra in the range of 100 cm^{-1} to 1200 cm^{-1} of the glasses in samples C2, C1, C3, D7, C8b, D6, and D5 from the top with decreasing SiO_2 concentrations from 97 wt.% (top spectrum, C2) to 0.5 wt. (bottom spectrum D5).

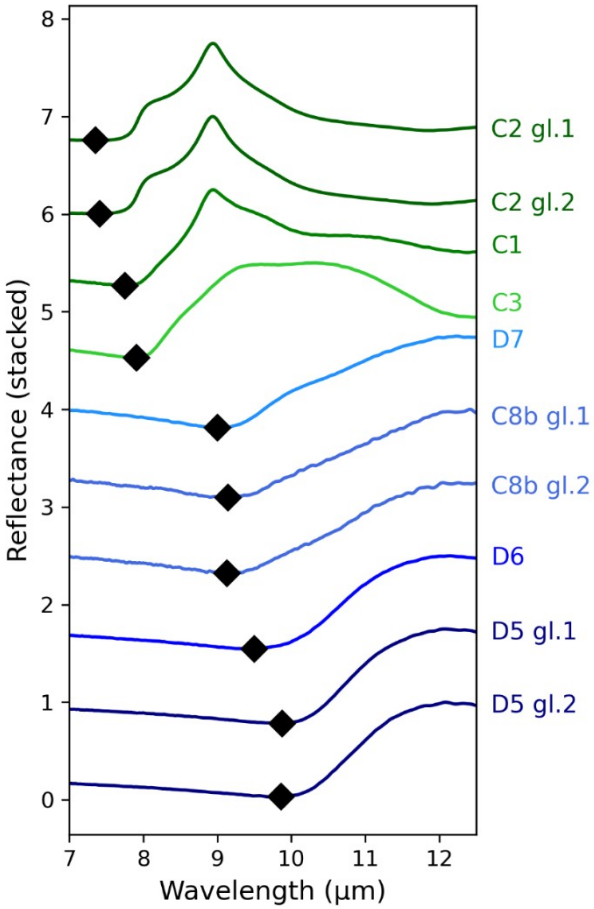

Figure S3. Mid-infrared spectra in the range of 7 µm to 13 µm of the measured glasses from the top with decreasing SiO_2 concentrations from 97 wt.% (top spectrum, C2) to 0.5 wt. (bottom spectrum D5). The color-coding of the spectra is the same as for the indicated areas on the SEM images in Figure S1. The black diamonds indicate the positions of the CF, which are the reflectance minima.

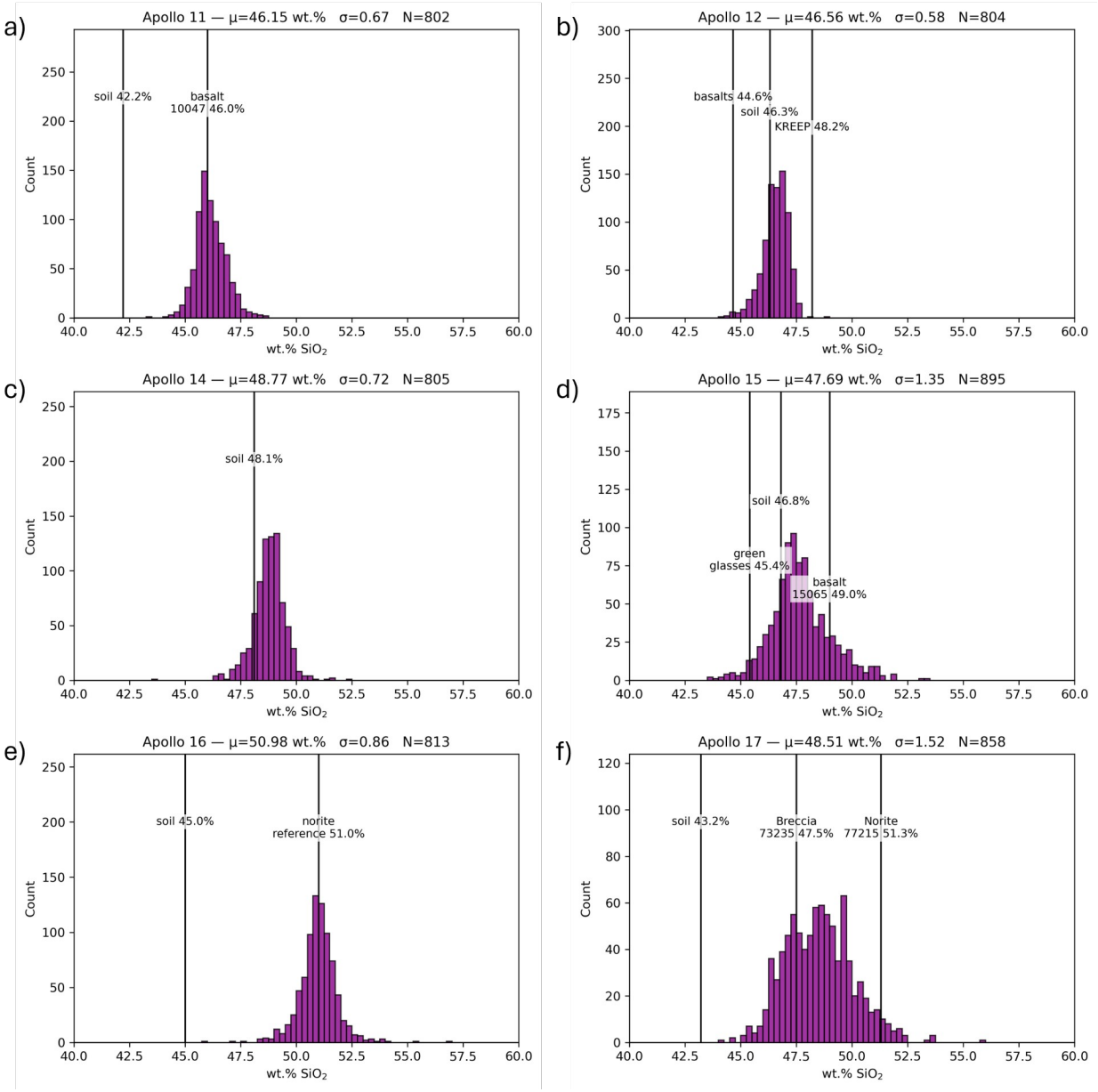

Figure S4. Comparison of calculated SiO_2 wt.% concentrations at the Apollo landing sites a) Apollo 11; b) Apollo 12; c) Apollo 14; d) Apollo 15; e) Apollo 16; f) Apollo 17. The histograms show the SiO_2 abundances at the landing sites over an area of 0.5° for reliable counting statistics (Table S3). For comparison we include the compositions of representative returned Apollo samples from literature compilations by Heiken et al. (1991), and the Lunar Sample Compendium (2012).

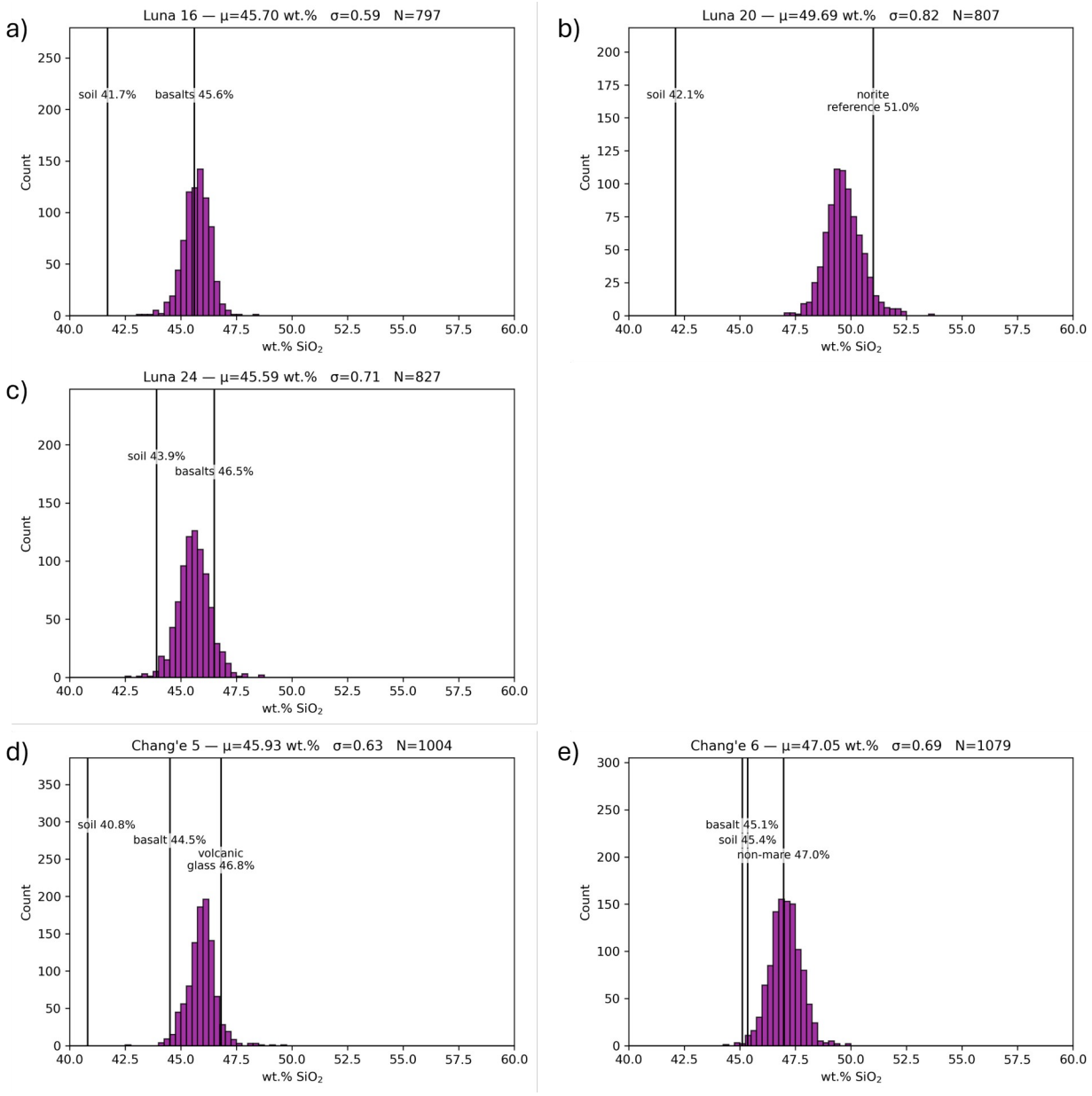

Figure S5. Comparison of calculated SiO_2 wt.% concentrations at the Luna landing sites a) Luna 16; b) Luna 20; c) Luna 24, and the Chang'e landing sites d) Chang'e 5; e) Chang'e 6. The histograms show the SiO_2 abundances at the landing sites over an area of 0.5° for reliable counting statistics (Table S3) For comparison we include the compositions of representative returned samples by the Luna missions (Keil et al., 1972; Taylor et al., 1978), and the Chang'e missions (Boschi et al., 2023, Che et al., 2021; Li et al., 2022; Li et al., 2024; B.-W. Wang et al., 2024, Wang et al., 2025, Zong et al., 2022).

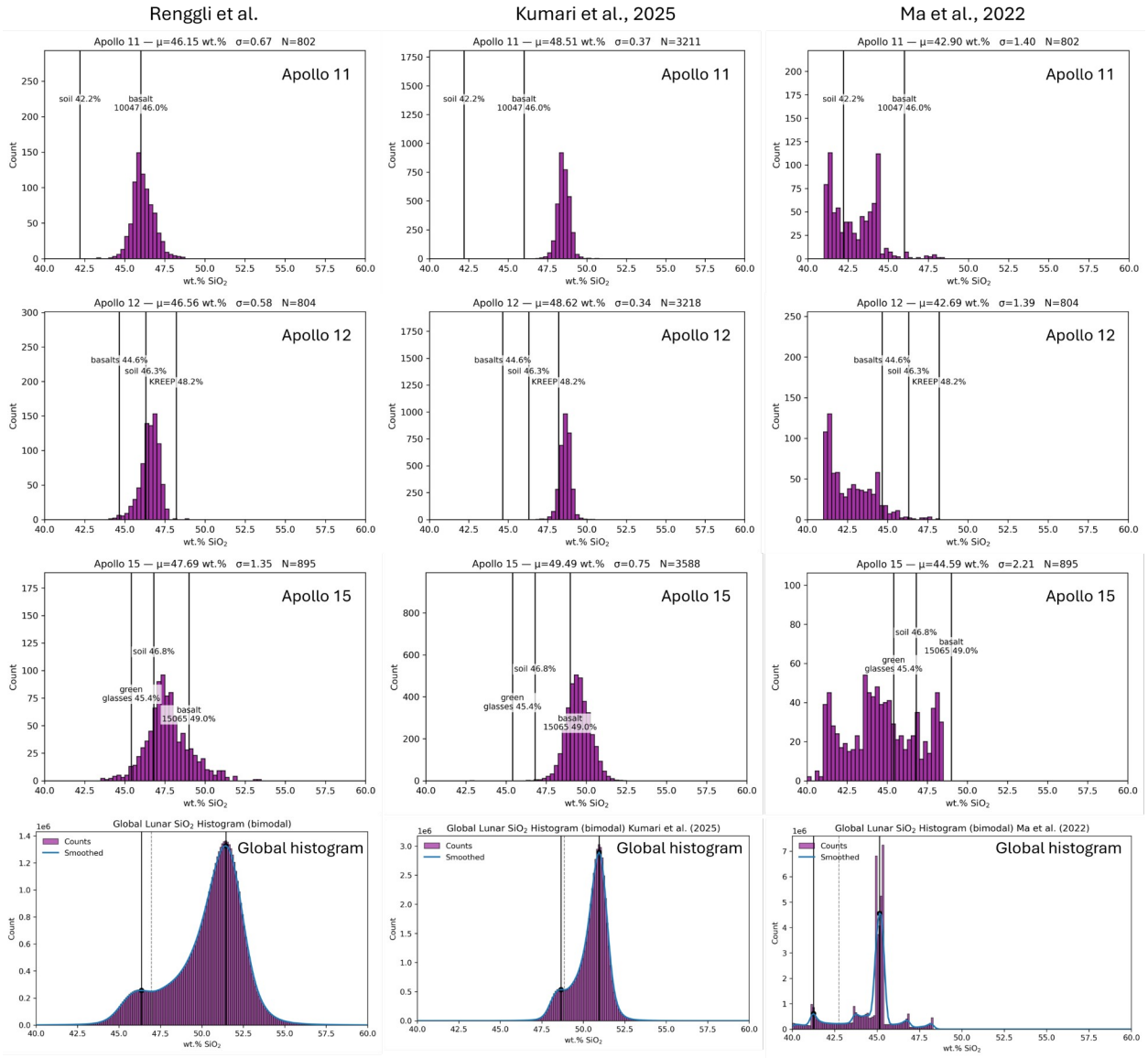

Figure S6. Comparison of calculated SiO_2 wt.% concentrations with our new calibration (left column), for the linear CF-SiO_2 relationship by Kumari et al. (2025) applied to the same CF dataset by Lucey et al., (2021) (middle column), and the SiO_2 dataset by Ma et al. (2022) (right column). The top row shows the histograms for the region of the Apollo 11 landing sites, the second row for Apollo 12, the third row for Apollo 15, and the bottom row the respective global SiO_2 histograms. The calibration based on Kumari et al. (2025) results in systematically overestimated SiO_2 concentrations, whereas the model by Ma et al. (2022) shows unnatural distributions which also tend to be too low.